Reports of the Department of Geodetic Science and Surveying

Report No. 376

Spherical Harmonic Expansions of the Earth's Gravitational Potential To Degree 360 Using 30' Mean Anomalies

by

Richard H. Rapp

and

Jaime Y. Cruz

Prepared for

National Aeronautics and Space Administration
Goddard Space Flight Center
Greenbelt, Maryland 20770

NASA Grant No. NGR 36-008-161
OSURF Project 783210

The Ohio State University
Department of Geodetic Science and Surveying
1958 Neil Avenue
Columbus, Ohio 43210-1247

December 1986

Abstract

Two potential coefficient fields that are complete to degree and order 360 have been computed. One field (OSU86E) excludes geophysically predicted anomalies while the other (OSU86F) includes such anomalies. These fields were computed using a set of 30' mean gravity anomalies derived from satellite altimetry in the ocean areas and from land measurements in North America, Europe, Australia, Japan and a few other areas. Where no 30' data existed, 1°x1° mean anomaly estimates were used if available. No rigorous combination of satellite and terrestrial data was carried out. Instead we took advantage of the adjusted anomalies and potential coefficients from a rigerous combination of the GEML2' potential coefficient set and 1°x1° mean gravity anomalies.

The two new fields were computed using a quadrature procedure with de-smoothing factors suggested by Colombo. The spectra of the new fields agree well with the spectra of the fields with 1°x1° data out to degree 180. Above degree 180 the new fields have more power. The fields have been tested through comparison of Doppler station geoid undulations with undulations from various geopotential models. The agreement between the two types of undulations is approximately ±1.6 m. The use of a 360 field over a 180 field does not significantly improve the compariosn. Instead it allows the comparison to be done at some stations where high frequency effects are important. In addition maps made in areas of high frequency information (such as trench areas) clearly reveal the signal in the new fields from degree 181 to 360.

Foreword

This report was prepared by Richard H. Rapp, Professor, and Jaime Y. Cruz, Post-Doctoral Researcher, Department of Geodetic Science and Surveying, The Ohio State University, under NASA Grant NGR36-008-161, The Ohio State University Research Foundation Project No. 783210. The grant covering this research is administered through the NASA Goddard Space Flight Center, Greenbelt Maryland 20771. The NASA Technical Officer for this grant is Mr. Jean Welker, Code 621.

Some computer funds for the research described here were supplied through the Instruction and Research Computer Center.

The reproduction and distribution of this report was carried out with funds supplied, in part, by the Department of Geodetic Science and Surveying.

1. Introduction

This report describes our first attempt at carrying out a spherical harmonic expansion of the earth's gravity field to degree and order 360. The procedure followed is built on an adjustment of satellite derived potential coefficients and 1°x1°. mean gravity anomalies that is described by Rapp and Cruz (1986). This combination solution yielded a set of potential coefficients corresponding to those values with a priori information, and a set of adjusted 1°x1° anomalies. These anomalies were then used in a least squares collocation estimation procedure to determine a set of potential coefficient to degree 250. Examination of the spectrum of this field led to the suggestion that smoothing was taking place at the higher degrees due to the averaging in the 1°x1° cells.

In order to estimate more reliable high degree fields we decided to use anomalies in smaller block sizes--specifically 30'x30' anomalies. A rigorous repeat of the prior adjustment was not possible so that an alternate procedure was developed to obtain an expansion to degree 360. The following sections describe the methods used and the results obtained.

2. The Previous Combination Solution

In this section we briefly review the procedures that were followed by Rapp and Cruz (1986). The starting equation is the expression for the gravitational potential written in the following form:

$$V(r,\phi,\lambda) = \frac{kM}{r}\left[1 + \sum_{\ell=2}^{\infty}\left(\frac{a}{r}\right)^{\ell}\sum_{m=0}^{\ell}(\bar{C}_{\ell m}\cos m\lambda + \bar{S}_{\ell m}\sin m\lambda)\bar{P}_{\ell m}(\sin\phi)\right] \qquad (1)$$

where:

r,ϕ,λ	geocentric coordinates
kM	geocentric gravitational constant
a	equatorial radius of the reference ellipsoid
$\bar{C}_{\ell m},\bar{S}_{\ell m}$	fully normalized potential coefficients
$\bar{P}_{\ell m}$	fully normalized Legendre function of degree ℓ and order m.

The disturbing potential can be written as:

$$T(r,\phi,\lambda) = \frac{kM}{r} \sum_{\ell=2}^{\infty} \left(\frac{a}{r}\right)^{\ell} \sum_{m=0}^{\ell} \sum_{\alpha=0}^{1} \bar{C}_{\ell m}^{\alpha} \bar{Y}_{\ell m}^{\alpha}(\phi,\lambda) \qquad (2)$$

where:

$$\bar{C}_{\ell m}^{\alpha} = \begin{cases} \bar{C}_{\ell m}, & \alpha=0 \\ \bar{S}_{\ell m}, & \alpha=1 \end{cases}$$

$$\bar{Y}_{\ell m}^{\alpha}(\phi,\lambda) = \begin{cases} \bar{P}_{\ell m}(\sin\phi)\cos m\lambda, & \alpha=0 \\ \bar{P}_{\ell m}(\sin\phi)\sin m\lambda, & \alpha=1 \end{cases} \qquad (3)$$

The gravity anomaly, in the Molodensky surface free-air anomaly sense is given as:

$$\Delta g_P = g_P - \gamma_Q \qquad (4)$$

where P is at the surface and Q is on the telluroid. The boundary condition that relates Δg and T is as follows:

$$\Delta g = -\frac{\partial T}{\partial h} + \frac{1}{\gamma}\frac{\partial \gamma}{\partial h} T \qquad (5)$$

where h is the plumbline direction. Neglecting deflections of the vertical equation (2) can be substituted into (5) to obtain:

$$\Delta g = \frac{kM}{r^2} \sum_{\ell=2}^{\infty} (\ell-1)\left(\frac{a}{r}\right)^{\ell} \sum_{m=0}^{\ell} \sum_{\alpha=0}^{1} (\bar{C}_{\ell m}^{\alpha} - \bar{C}_{\ell m}^{\alpha,h} - \bar{C}_{\ell m}^{\alpha,\gamma}) \bar{Y}_{\ell m}^{\alpha}(\phi,\lambda) \qquad (6)$$

where $\bar{C}_{\ell m}^{\alpha,i}$ $(i=h,\gamma)$ are ellipsoidal corrections. If we assume that we have the anomalies (Δg) given on the surface of the reference ellipsoid equation (6) can be inverted to solve for potential coefficients (Cruz, 1986). We have:

$$\bar{C}_{\ell m}^{\alpha} = \bar{C}_{\ell m}^{\alpha,o} + \bar{C}_{\ell m}^{\alpha,h} + \bar{C}_{\ell m}^{\alpha,\gamma} + \bar{C}_{\ell m}^{\alpha,1} + \bar{C}_{\ell m}^{\alpha,2} + \bar{C}_{\ell m}^{\alpha,3} \qquad (7)$$

In (7) we have:

$$\bar{C}_{\ell m}^{\alpha,o} = \frac{1}{\frac{kM}{a^2}(\ell-1)} \frac{1}{4\pi} \int_{\sigma}\int \Delta g_E \bar{Y}_{\ell m}^{\alpha}(\phi,\lambda) d\sigma \qquad (8)$$

The other terms in (7) are ellipsoidal correction terms defined in Rapp and Cruz (ibid, pp. 16-17).

The gravity anomaly on the ellipsoid must be determined by downward continuing the surface anomaly to the ellipsoid and adding an atmospheric correction (δg_A). We have used the following:

$$\Delta g_E = \Delta g_S + \delta g_A - \frac{\partial \Delta g}{\partial r} h - \frac{1}{2!} \frac{\partial^2 \Delta g}{\partial r^2} h^2 \qquad (9)$$

This downward continuation is an approximation. For our work the derivatives were calculated from an expansion to degree 300 which was developed as part of a previous solution (Rapp, 1981).

The combination solution was carried out through the adjustment of the potential coefficients derived from satellite analysis and the coefficients implied by gravity data. Specifically the mathematical model, F, was taken as

$$F = L_X a - L_{X_C} a = 0 \qquad (10)$$

where $L_X a$ is the adjusted potential coefficient set derived from satellite data and $L_{X_C} a$ is the potential coefficient set implied by the adjusted gravity anomalies given in cells on the earth. The linearization of (10) is written:

$$B_\ell V_\ell + B_X V_X + W = 0 \qquad (11)$$

where V_ℓ are corrections to the approximate anomalies, and V_X are corrections to the a priori known potential coefficients. The W vector is:

$$W = L_X o - L_{X_o} c \qquad (12)$$

where $L_X o$ is the approximate potential coefficient set and $L_{X_o} c$ is the potential coefficient set implied by "observed" anomalies. The model is formulated taking into account ellipsoidal corrections and downward continuation effects. We start this by computing the $\bar{C}^{\alpha,o}_{\ell m}$ values from the given potential coefficient using (7). We have:

$$\bar{C}^{\alpha,o}_{\ell m} = L_X o = \bar{C}^{\alpha}_{\ell m} - \Delta \bar{C}^{\alpha,o}_{\ell m} \qquad (13)$$

where $\Delta \bar{C}^{\alpha,o}_{\ell m}$ are all but the first terms on the right side of (7). Using equation (8) the values of $L_{X_o} c$ are computed.

The adjustment is now carried out to obtain V_X and V_ℓ. Specifically:

$$V_X = - ((B_\ell \, P_{\bar{\ell}}^{-1} \, B_\ell^T)^{-1} + P_X)^{-1} \, (B_\ell \, P_{\bar{\ell}}^{-1} \, B_\ell^T)W \tag{14}$$

$$V_\ell = P_{\bar{\ell}}^{-1} \, B_\ell^T \, P_X \, V_X \tag{15}$$

P_ℓ is the weight matrix of the observations and P_X is the weight matrix of the a priori potential coefficients. The elements in B_ℓ are given by the coefficients of Δg_E in equation (8). The adjusted potential coefficients, compatible with satellite derived estimates, would be:

$$\bar{C}^{\alpha}_{\ell m,a} = L_X o + V_X + \Delta \bar{C}^{\alpha,o}_{\ell m} \tag{16}$$

The adjusted anomalies on the ellipsoid would be:

$$L_\ell a = L_\ell o + V_\ell \tag{17}$$

while the adjusted anomalies at the surface of the earth would be found from equation (9).

In our combination solution we used the GEML2' potential coefficients that are very similar to the GEML2 coefficients described by Lerch et al. (1982). In addition we used a few additional coefficients to degree and order 30. The total number of coefficients estimated was 582.

The 1°x1° gravity anomaly data was based on the merger of terrestrial anomaly estimates with altimeter derived gravity anomalies. In this merger we considered two forms. One form excluded most geophysically predicted anomalies while the second form included such anomalies. In the first case we had a total of 50,562 1°x1° anomalies while in the second case there were 56,109 values. Figures 3 and 4 of Rapp and Cruz (ibid) show the location of these anomalies. In order to fill in the "empty" areas we computed the anomalies from the a priori potential coefficient set.

The higher degree potential coefficient fields were made by applying an optimal estimation procedure to the adjusted anomalies on the ellipsoid. This would correspond to a least squares collocation estimation using appropriate covariance functions, anomaly degree variance models, and anomaly accuracy estimates. The process of the optimal estimation as developed by Colombo (1981) with implementation for 1°x1° data described by Hajela (1984) requires, for a complete solution, extensive computations. The solution we estimated was to degree 250. After the coefficients are estimated it is necessary to <u>add</u> the $\Delta \bar{C}^{\alpha,o}_{\ell m}$ corrections introduced in equation (13).

It is possible to approximate the optimal estimate through the use of a modified orthogonality procedure. If the anomalies were given on the complete surface of the ellipsoid we could use (8) to compute $\bar{C}^{\alpha,o}_{\ell m}$. Since data are actually given in discrete cells an implementation of(8), to approximate an optimum estimation, was suggested by Colombo (1981). If the data is given in blocks of θ° let $N = 180^\circ/\theta^\circ$. Then we have:

$$\bar{C}^{\alpha,o}_{\ell m} = \frac{1}{4\pi\gamma(\ell-1)q_\ell} \sum_{i=o}^{N-1} \sum_{j=o}^{2N-1} \Delta\bar{g}_{ij} \int\int_{\sigma_{ij}} \bar{Y}^{\alpha}_{\ell m}(\phi,\lambda)\, d\sigma \qquad (18)$$

where: $\gamma = kM/a^2$;

$\Delta\bar{g}_{ij}$ = the mean anomaly corresponding to Δg_E;

$q_\ell = \beta_\ell^2$; $0 \leq \ell \leq N/3$

$q_\ell = \beta_\ell$; $N/3 < \ell \leq N$

$q_\ell = 1 \quad \ell > N$ (19)

β_ℓ is the Pellinen smoothing operator that depends on a circular cap radius which in turn depends on the size of the mean anomaly cell (Rapp and Cruz (ibid, p. 22)).

Using the adjusted 1°x1° mean anomalies of our combination solution we computed a set of potential coefficients from equation (18) which we have compared to the values from the optimal estimation solution. Table 1 (taken from Rapp and Cruz (ibid, Table 11) shows the differences in terms of undulations, anomalies, and percentage differences.

Table 1. Comparison of the Potential Coefficient Solution from Equation (18) with the Optimal Estimate Using 1°x1° Mean Anomalies.

ℓ	δN (cm)	δg(mgals)	P(%)
2	0.0	0.00	0.0
10	0.0	0.00	0.0
20	0.0	0.00	0.0
30	0.2	0.01	0.5
50	0.2	0.02	1.1
75	0.8	0.09	6.2
100	1.0	0.15	10.6
120	1.0	0.18	13.2
150	0.6	0.14	13.0
180	0.8	0.22	22.3
to 180	8.9	1.53	7.6

We see from this table that there is good agreement between the two solutions. The percentage differences are negligible at the lower degrees increasing to 22% at degree 180. The results from this test will be used later to justify the use of equation (18) with 30' mean anomalies instead of using the complicated optimal estimation results.

This section has been written to describe our potential coefficient solution using 1°x1° anomaly data and the GEML2' potential coefficients. The results of these computations were two potential coefficient sets computed using an optimal estimation procedure with a uniform data noise of one mgal for the anomalies. The solution that excludes geophysically predicted anomalies was designated OSU86C; the solution that included such anomalies was called OSU86D. Both solutions were complete to degree and order 250.

3. The 30'x30' Mean Anomaly Data Set

In order to extend the OSU86C/D solutions to a higher degree we first needed to put together a set of smaller anomaly cells in order to get the higher frequencies into our solution. The cell size chosen was 30'x30' although other sizes could be chosen. However this size is convenient to work with as four 30'x30' cells fill a 1°x1° cell.

The 30'x30' mean anomalies for the ocean areas had been computed by Rapp (1986) from Geos-3/Seasat altimeter data. Specifically computed were point anomalies on a 1/8° grid which were meaned to compute both 30' and 1° mean anomalies (and sea surface heights). The total number of predicted 30' anomalies was 149, 670 although about 1000 were considered unreliable because they were on land or in areas in which the altimeter data was sparse.

In order to obtain data from terrestrial estimates it was necessary to collect gravity anomaly data as point values or small (10'x10', 6'x10') mean values. Such values were then formed into 30'x30' values with individual accuracy estimates where possible. The development of this 30' terrestrial anomaly data base is described by Despotakis (1986). Figure 1 shows the location of the 30' mean anomalies in the August 1986 field.

We next created a merger of the altimeter derived anomalies and the terrestrial values. In the ocean areas we used the altimeter derived anomaly unless its standard deviation was greater than 30 mgals or if the anomaly was in a 1°x1° block whose elevation was greater than or equal to zero. For the remaining areas the 30' terrestrial values were used if they were available. The atmospheric correction (δg_A) was added to the terrestrial anomalies (see equation 9) and a gravity formula correction of -0.6 mgal was added to convert to our reference system of constants. If neither an altimeter derived anomaly nor terrestrial anomaly was available the adjusted 1°x1° anomaly from the combination solution was used as fill-in values.

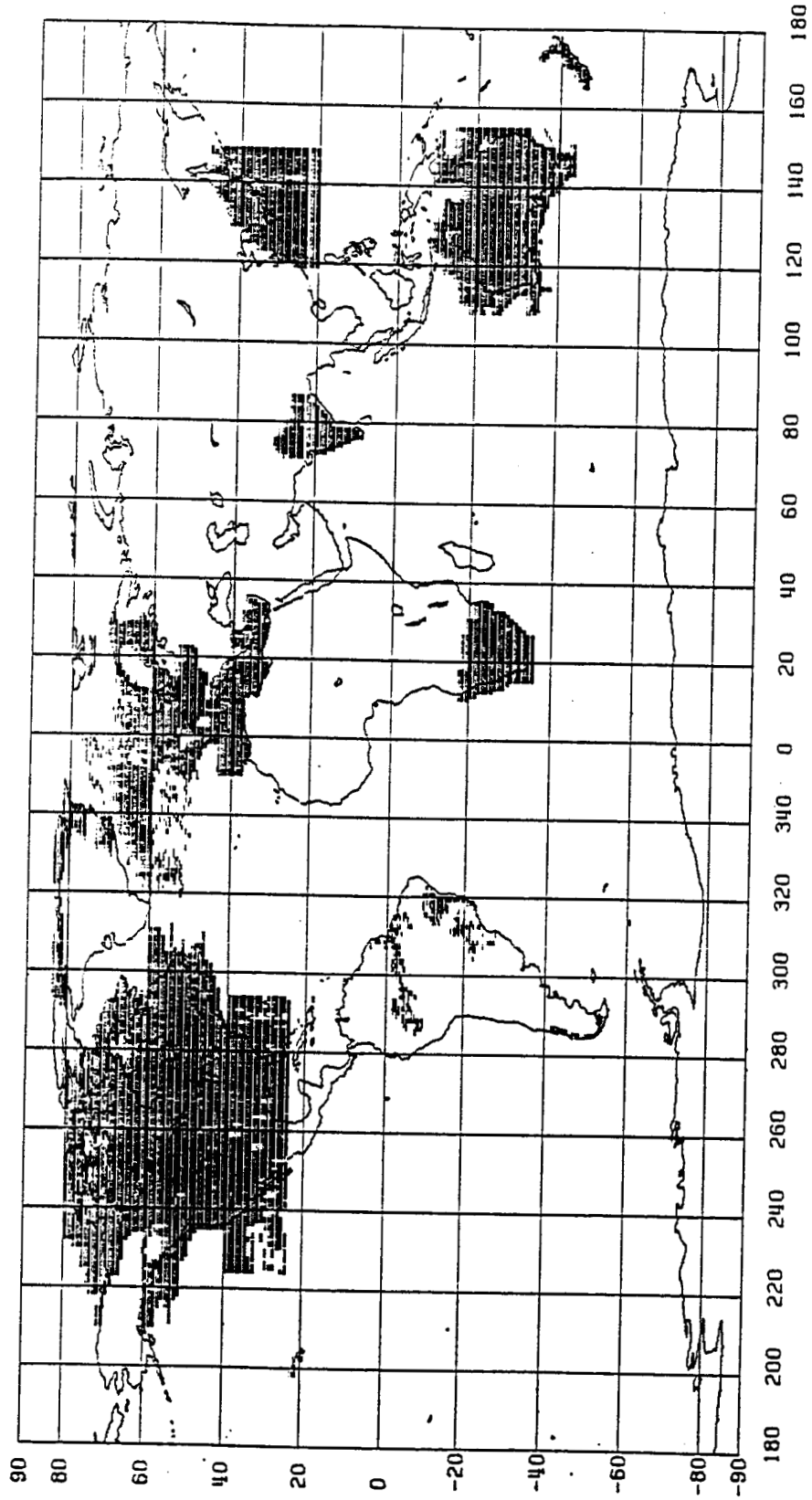

Figure 1. Location of 31450 30'x30 Mean Free Air Anomalies Estimated From Terrestrial Data

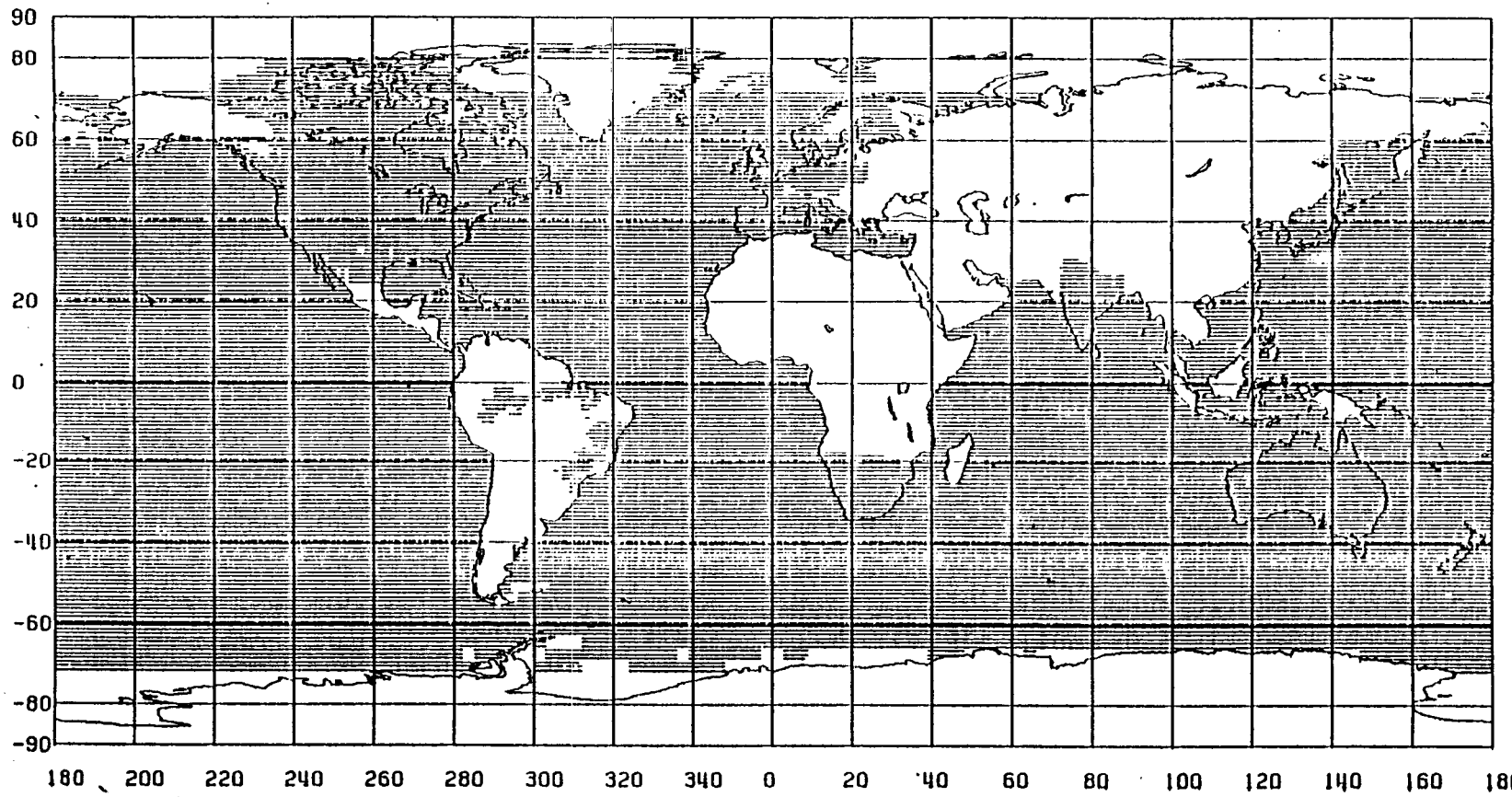

Figure 2. Location of 40700 1°x1° Cells with at least a single 30' value from the terrestrial or altimeter data set.

In order to take advantage of the least squares adjustment that led to the OSU86C/D solutions we took the adjusted 1°x1° values of these solutions and forced the mean of the four 30' values within the blocks to be the same by applying a bias term to each of the non-fill-in 30' values. Specifically we write:

$$B = \Delta g_E(1^\circ, A) - \frac{\Sigma \Delta g_S(30', UA)}{n} \qquad (20)$$

In (20) the A stands for adjusted and UA stands for unadjusted and n is the number (usually 4) of non-fill-in 30' values in the 1° blocks. The B term would consist of three effects: the downward continuation of the surface anomalies to the ellipsoid (see equation 9); the inconsistencies of the 30' and 1° values; and differences caused by the adjustment process. The B value for each 1° block was then added to the non-fill-in 30' value to obtain a value that we consider to be on the ellipsoid (Δg_E) and is consistent with the adjusted anomalies of our earlier solutions.

In summary the merger process used 139,946 values derived from altimeter data; 21,739 values from the terrestrial data, and 97,515 "fill-in" values from the adjusted 1°x1° data. The total number of 30' anomalies is 259,200. Figure 2 shows the location of 40700 1°x1° blocks in which at least one 30' value from either the altimeter derived or terrestrial data set was used.

4. The Estimation of the Potential Coefficients

If we were to start the combination process from our 30' data we would need to evaluate equations (14) and (15). This process is feasible with a vector processing machine. However we did not feel that the effort for such a solution was worthwhile at this time. Since the actual adjustment is done with the coefficients of the satellite solution, which was complete only to degree and order 20, we felt that whether this adjustment was made with 1° data or 30' data would be irrelevant. We consequently adopted the adjusted coefficients of the OSU86C/D solutions. For the other coefficients to degree 360 we used equation (18) through the HARMIN program of Colombo (1981) where the $\Delta\bar{g}_{ij}$ values were taken as the bias corrected 30' values. This computation required an evaluation of the integrals of the fully normalized associated Legendre functions up to degree and order 360 at 30' intervals. This was done using program F428AV1 which implements the Paul (1978) subroutine with changes suggested by Gleason (1985).

The HARMIN program (OSU program F419B) was used with the q_ℓ factors given by equation (19). Two solutions to degree 360 were carried out. The OSU86E solution basically excluded geophysically predicted anomalies while the OSU86F solution included such anomalies. After the potential coefficients from equation (18) were found, the ellipsoidal corrections given by $\Delta\bar{C}^{\alpha,\circ}_{\ell m}$ of equation (13) were applied. These corrected coefficients were then merged with the adjusted and corrected coefficients of the OSU86C or D solution to form the final potential coefficient sets.

5. Potential Coefficient Accuracy

One disadvantage of using the HARMIN approach to the potential coefficient estimation is the lack of estimated coefficient accuracies. In fact, the use of the more rigorous optimal estimation procedure does not ensure realistic accuracies because of the smoothing of the field that takes place at the higher degrees when realistic anomaly standard deviations are used. To avoid this problem Rapp and Cruz (ibid) combined the sampling error (from the optimal estimation procedure) with a propagated noise assuming uncorrelated anomaly errors of 10 mgal. This procedure led to a noise magnitude that was equal to the signal near degree 175 (see Figure 3). Since we do not have a formal sampling error estimate for the 30' solution, and since the assumption of uncorrelated 30' anomaly errors is even more unrealistic than the 1° case we have not computed the potential coefficient errors for the OSU86E and F solutions. If there are requirements that demand coefficient accuracy estimates for the 86E/F fields, we suggest the use of the 86C/D standard derivation to degree 175 followed by a 100% uncertainty in the coefficients above that degree.

6. Anomaly Degree Variances

We first define the spectrum or power at degree ℓ as follows:

$$\sigma_\ell = \sum_{m=0}^{\ell} (\bar{C}_{\ell m}^2 + \bar{S}_{\ell m}^2) \tag{21}$$

The anomaly degree variances, c_ℓ are given as:

$$c_\ell = \gamma^2(\ell-1)^2\sigma_\ell \tag{22}$$

where $\gamma = kM/a^2$. The anomaly degree variances are formally given on a sphere of radius a. Figure 3 shows the anomaly degree variances for the OSU86C and the OSU86E solution. Also shown is the accuracy estimate of the OSU86C solution based on the optimal estimation procedure with an anomaly standard deviation of one mgal and a propagated standard deviation of 10 mgal for the 1°x1° anomalies (Rapp and Cruz, ibid, equation (6.11)). We see that the power is almost identical in the two solutions out to degree 200 although OSU86C solution shows slightly less power between degrees 120 and 160. Beyond degree 204, out to degree 250, the 86C solution has power that falls off much more rapidly than the solution (OSU86E) with the 30' anomalies. This seems to reflect the loss of information, not recovered by the optimal estimation procedure, in the 1° averaging process. This might imply that the rough rule of thumb (180°/θ°, θ° = block size) for how high a degree should a spherical harmonic expansion be taken may not be unreasonable.

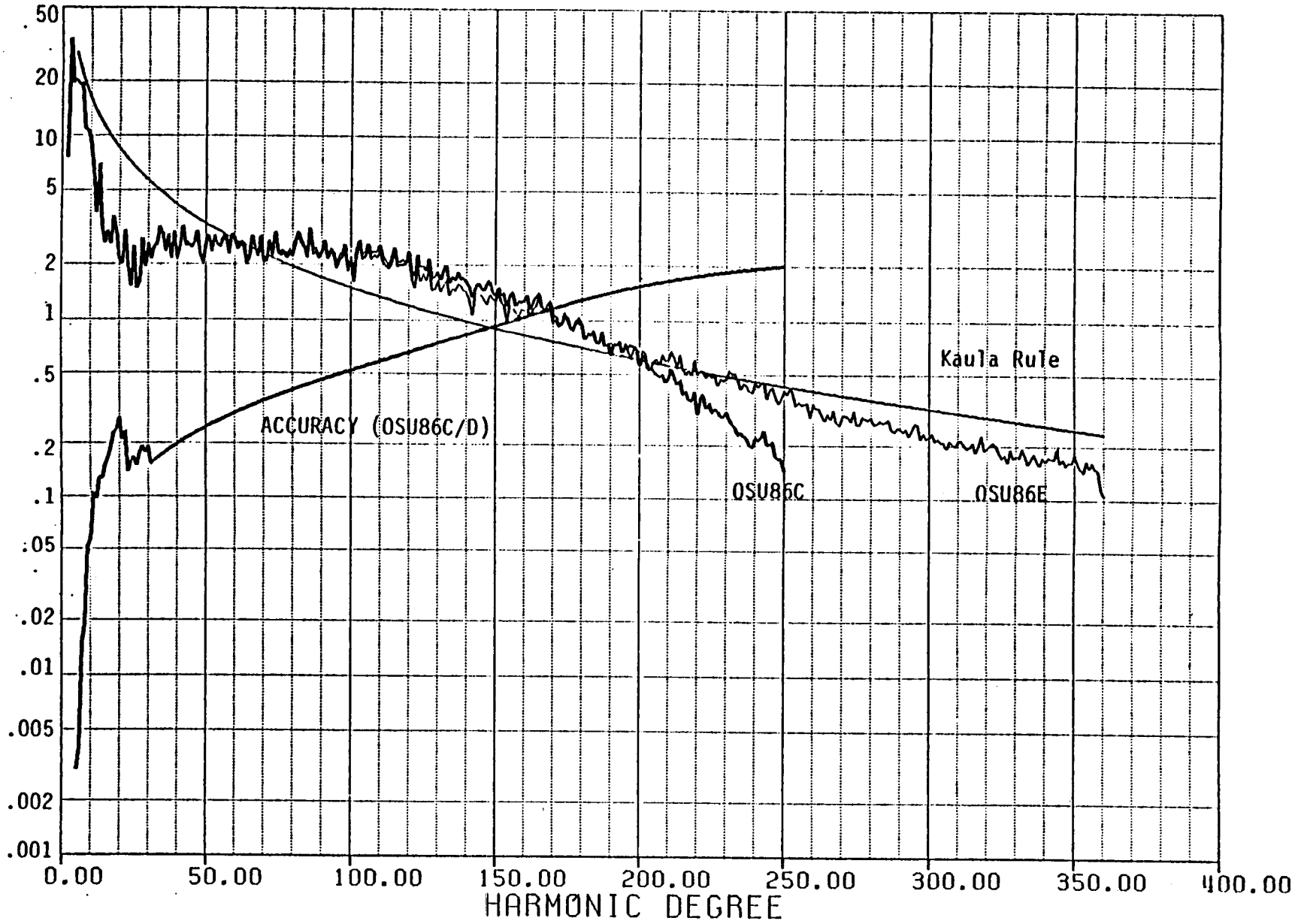

Figure 3. Anomaly Degree Variances for OSU86C (1°, no geophysical anomalies) and OSU86E (30', no geophysical anomalies); Error Anomaly Degree Variances for OSU86C; and Anomaly Degree Variances from Kaula's Rule.

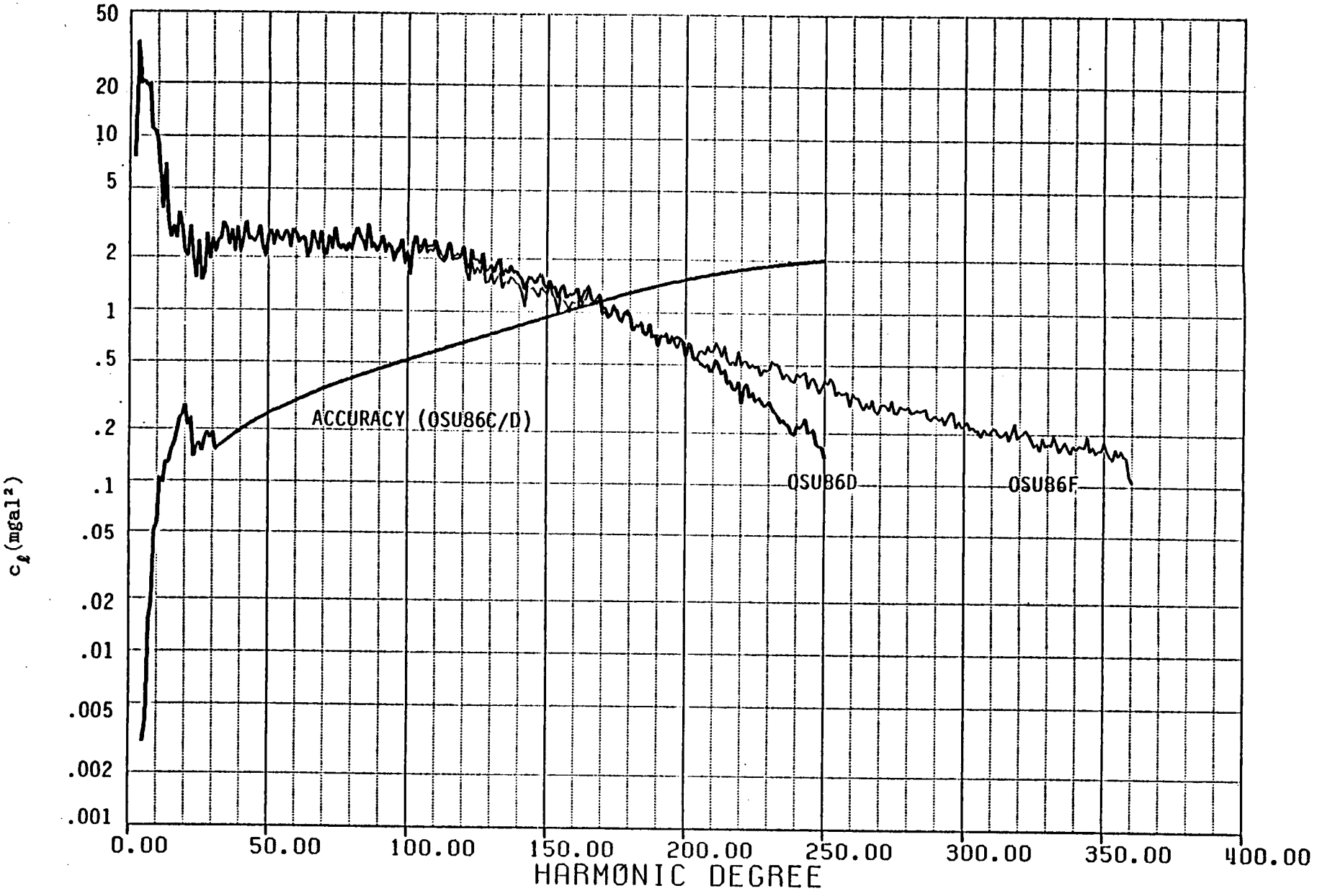

Figure 4. Anomaly Degree Variances for OSU86D (1°, with geophysical anomalies) and OSU86F (30', with geophysical anomalies); Error Anomaly Degree Variances for OSU86C/D.

Figure 3 also shows the anomaly degree variance implied by the Kaula rule for the decay of potential coefficients (i.e. the $10^{-5}/\ell^2$ rule). The anomaly degree variance implied by this rule has been computed on a sphere of radius a assuming the original rule was based on data referred to the mean surface of the earth. Specifically plotted was:

$$c_\ell(a) = \frac{192}{\ell+1.5}\left(\frac{R_E}{a}\right)^{n+2} \text{mgal}^2 \qquad (23)$$

where R_E = 6371 km and a = 6378 km. The rule has too much power between degrees 10 to 50 and too little power between degrees 80 to 200. Beyond 200 the estimates from the model and from OSU86E are within 50% of each other.

Figure 4 shows the anomaly degree variances for the OSU86D (1°) and the OSU86F (30') solutions. Both these solutions used the geophysically predicted anomalies. Also shown is the accuracy of the OSU86C/D solutions. The comments made with respect to the anomaly degree variances shown in Figure 3 are also applicable here.

Specific values of the anomaly degree variances, at selected degrees, for the four solutions discussed here are given in Table 2.

Table 2. Anomaly Degree Variances. (Units are mgal^2).

Degree	Solution			
ℓ	OSU86C	OSU86E	OSU86D	OSU86F
50	2.66	2.57	2.94	2.83
100	2.23	2.13	2.35	2.23
150	1.36	1.28	1.48	1.33
180	0.96	0.97	1.02	1.01
200	0.57	0.60	0.56	0.61
250	0.14	0.41	0.16	0.43
300		0.22		0.22
350		0.18		0.18

From this table we see that there is no substantial difference, at the higher degrees, in the power of the OSU86E and F solutions.

7. Doppler Undulation Comparisons

As discussed by Rapp and Cruz (ibid, section 8.3) the accuracy of a potential coefficient model may be judged by comparing the geoid undulation derived from the model and the value implied by the ellipsoidal and orthometric heights at a station. This can only be done after the station coordinates have been converted to a geocentric, true scale system, and the

best estimate of the equatiorial radius is used.

We carried out these computations with the new models for a global Doppler station set, and data sets in North America, Australia and in Europe. In these tests an equatorial radius of 6378136 m was used. the mean difference (Doppler minus model) and the standard deviation of the difference is given in Table 3 for Europe, and Table 4 for Australia for a fixed number of stations.

Table 3. Comparison of Doppler Derived Undulations in Europe With Values From Models. 173 Stations Used.

Model	ℓ(max)	Mean Difference	Std Dev Difference
OSU81	180	-.04 m	±1.51 m
GPM2	180	-.28	1.47
OSU86C	180	-.47	1.38
OSU86D	180	-.39	1.42
OSU86E	180	-.48	1.35
OSU86E	360	-.50	1.33
OSU86F	180	-.40	1.38
OSU86F	360	-.42	1.36

Table 4. Comparison of Doppler Derived Undulations in Australia With Values From Models. 114 Stations Used.

Model	ℓ(max)	Mean Difference	Std Dev Difference
OSU81	180	-1.18 m	±1.57 m
GPM2	180	-0.96	1.51
OSU86C	180	-1.13	1.60
OSU86D	180	-1.12	1.60
OSU86E	180	-1.13	1.58
OSU86E	360	-1.10	1.57
OSU86F	180	-1.12	1.58
OSU86F	360	-1.09	1.57

From these two tables we see that in Europe, of the degree 180 solutions the OSU86E is best, while in Australia GPM2 is the best. The degree 360 fields in Europe show a slight improvement over their 180 counterparts. In Australia the 360 fields are slightly better than the 180 fields with the exception of GPM2 which fits the best for this area.

For North America and the global data set we carried out the comparisons rejecting stations where the residual was greater than 4 m. Therefore in

judging the results of these comparisons we consider the standard deviation and the number of stations accepted for the comparison. These results are shown in Table 5, for North America, and in Table 6, globally.

Table 5. Comparison of Doppler Derived Undulations in North America With Values from Models

Model	ℓ(max)	Mean Difference	Std Dev Difference	Num of Stations
OSU81	180	0.22	±1.72 m	683
GPM2	180	0.18	1.58	695
OSU86C	180	0.20	1.54	687
OSU86D	180	0.26	1.55	687
OSU86E	180	0.21	1.52	689
OSU86E	360	0.26	1.45	695
OSU86F	180	0.28	1.52	688
OSU86F	360	0.31	1.47	696

Table 6. Comparison of Doppler Derived Undulations Globally With Values From Models.

Model	ℓ(max)	Mean Difference	Std Dev Difference	Num of Stations
OSU81	180	0.18 m	±1.76 m	1721
GPM2	180	0.13	1.64	1735
OSU86C	180	0.17	1.66	1741
OSU86D	180	0.21	1.66	1743
OSU86E	180	0.16	1.67	1752
OSU86E	360	0.17	1.66	1777
OSU86F	180	0.21	1.66	1754
OSU86F	360	0.21	1.66	1780

From Table 5 we see, of the 180 solutions, both the OSU86E/F solutions give essentially the same results. Improved results are found with the 360 solutions with a small decrease in the standard deviation of fit and a small increase in the number of stations accepted.

From Table 6 we see all the solutions except the OSU81 solution give about the same standard deviation of fit. Of the 180 solutions, the OSU86F solution accepts the most stations. Of the two 360 solutions tested the OSU86F solution accepts the most stations.

In judging these results we must recall that the accuracy of the Doppler derived undulations may not be sufficient to distinguish the accuracy of various models at or below the ±1.5 m level. More accurate results might be obtained using laser station coordinates. Unfortunately such stations are

much fewer than the Doppler stations and they are located at difficult locations (e.g. mountain tops).

Rapp and Cruz (ibid, Section 8.4) discussed the undulation residual correlation with topography. Such correlation continues for these 360 fields. For example for the OSU86F field to degree 360, with the global station set, the slope is (0.41±.14) m/km with 1780 stations accepted. The value for the OSU86D field to degree 180 is (0.41±.12) m/km with 1741 stations accepted.

8. High Degree Geoid Maps

It would be possible, but not really meaningful, to compute a global geoid undulation map using the two new potential coefficient models to degree 360. Such maps would not be meaningful because the high degree contributions to the undulation, for the most part, are quite small. To first estimate the magnitude of the high degree terms we computed, for selected degrees, the undulation contribution from degrees ℓ+1 to degree ℓ_{max}. Values for selected degrees are given in Table 7.

Table 7. Geoid Undulation Magnitudes for Selected Degree Ranges in the OSU86F Model

Degree Range	Undulation Contribution
180 to 250	±20.2 cm
181 to 360	23.2 cm
251 to 300	9.3 cm

The values given in Table 7 represent global averages. To see specific estimates of the contribution made by the higher degree terms, we prepared two maps showing the geoid undulations computed from the coefficients from degree 181 to 360. Figure 5 shows this map for a region in the United States covering a portion of the Rocky Mountains. Figure 6 shows these effects for a region over the Tonga Trench.

In the Rockies test we can see effects that reach 1.8 m. In the Tonga Trench area the high frequency signal over the trench is clearly visible in the lineated pattern. The largest values are on the order of 2 meters. The latter case shows how the high degree fields can play a role where high frequency information is present in the gravity field. Note from Figure 6 that, outside the trench the contributions of the higher frequencies are quite small, approaching, it is speculated, the ±23 cm computed for Table 7.

Forsberg (1986) has computed the geoid undulation information above degree 180 based on power spectral analysis of gravity anomalies in Norway, Sweden, Finland and Denmark. Averaging over 37 2°x4° areas the information above degree 180 is ±32 cm with uncorrected anomaly data and ±28 cm with terrain corrected anomaly data. These values compare well with the ±23 cm value given in Table 7 when the summation is taken just to degree 360.

Figure 5. Geoid Undulations in a Rocky Mountain Region from Degrees 181 to 360 of the OSU86E Solution. The contour interval is 0.5 m. The data grid was 0.°25.

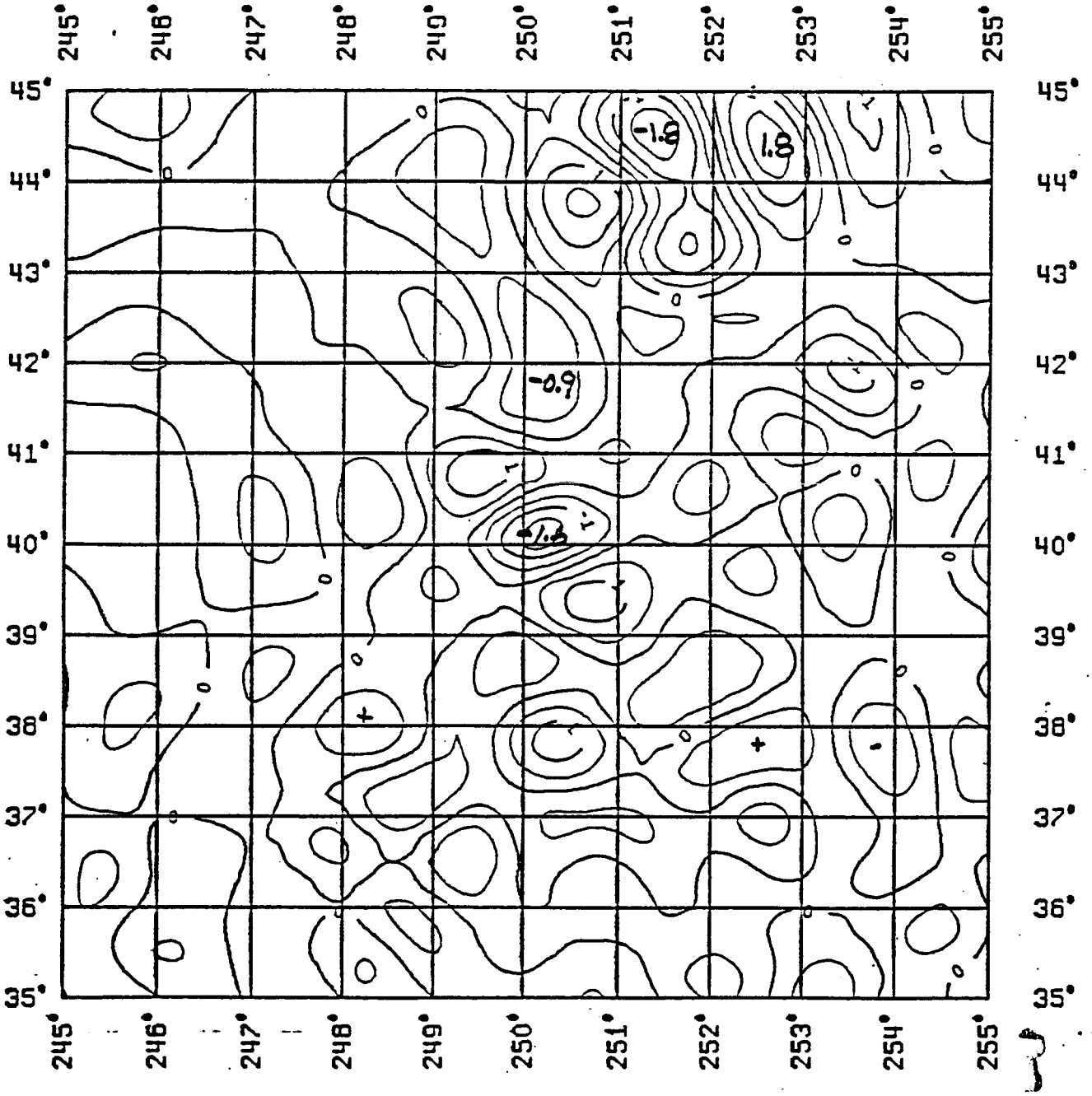

Figure 6. Geoid Undulations in the Tonga Trench Area from Degrees 181 to 360 of the OSU86E Solution. The contour interval is 0.5 m. The data grid was 0.°25.

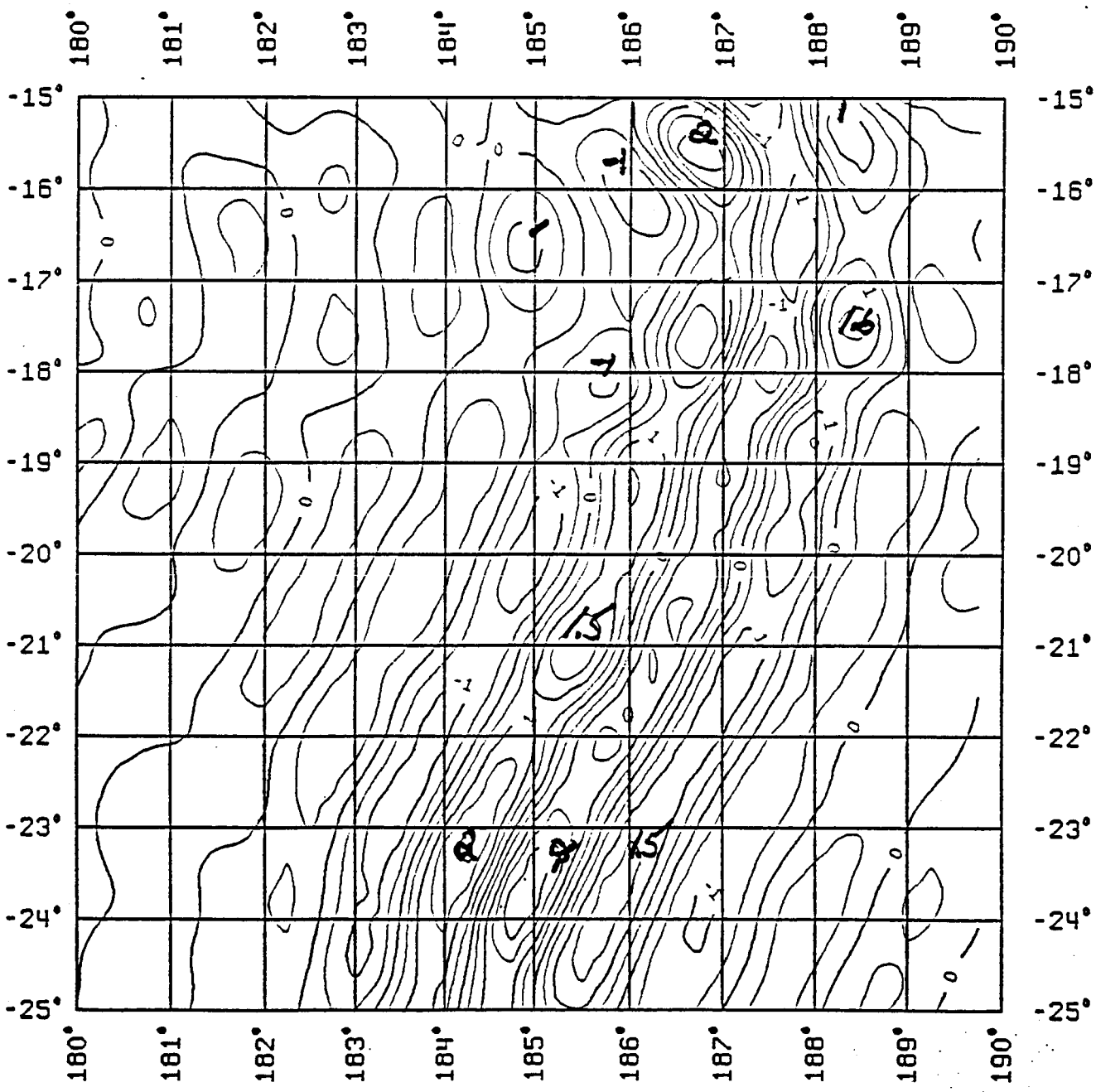

9. Coefficient Comparisons

It is of interest to compare the potential coefficients of the C/D solution with coefficients of the E/F solution up to degree 180. The C vs E comparison is given in Table 8 while the D/F comparison is given in Table 9.

Table 8. A Comparison of the OSU86C and E Models at Selected Degrees

ℓ	δN(cm)	δg(mgals)	Percent Diff.
50	0.7	0.05	3.3
75	0.9	0.11	6.9
100	1.2	0.18	11.9
120	1.4	0.26	17.2
150	1.7	0.38	33.0
180	1.8	0.49	50.2
2 to 180	15.7	3.18	14.6

Table 9. A Comparison of the OSU86D and F Models at Selected Degrees

ℓ	δN(cm)	δg(mgals)	Percent Diff.
50	0.8	0.06	3.5
75	1.0	0.11	6.9
100	1.2	0.18	11.7
120	1.5	0.27	17.9
150	1.7	0.40	32.8
180	1.8	0.49	48.9
2 to 180	16.1	3.25	14.6

The main thing that we see from these two tables is that the differences between the 1° and 30' data solutions are small up to degree 180. The differences are a function of degree, with the largest differences occuring at the higher degrees. This gives us some confidence in the 1° solutions but it also shows us the coefficients at the higher degrees may change by 50% from a 1° solution to a 30' solution. It would not be unreasonable to expect the coefficients at the high degrees of the E/F fields to change by this amount if 0.°25 anomalies were used instead of 0.°5 values.

As a last comparison we show in Figure 6 the undulation differences between the OSU86F and the OSU81 solutions up to degree 180. The contour map has been created from data given on a 2°x2° grid so that some high frequency differences may be missing. The maximum difference is 9.7 m which occurs in the southwest part of Africa. Most of the large undulation changes are due to substantial anomaly differences in the solutions.

ORIGINAL PAGE IS
OF POOR QUALITY

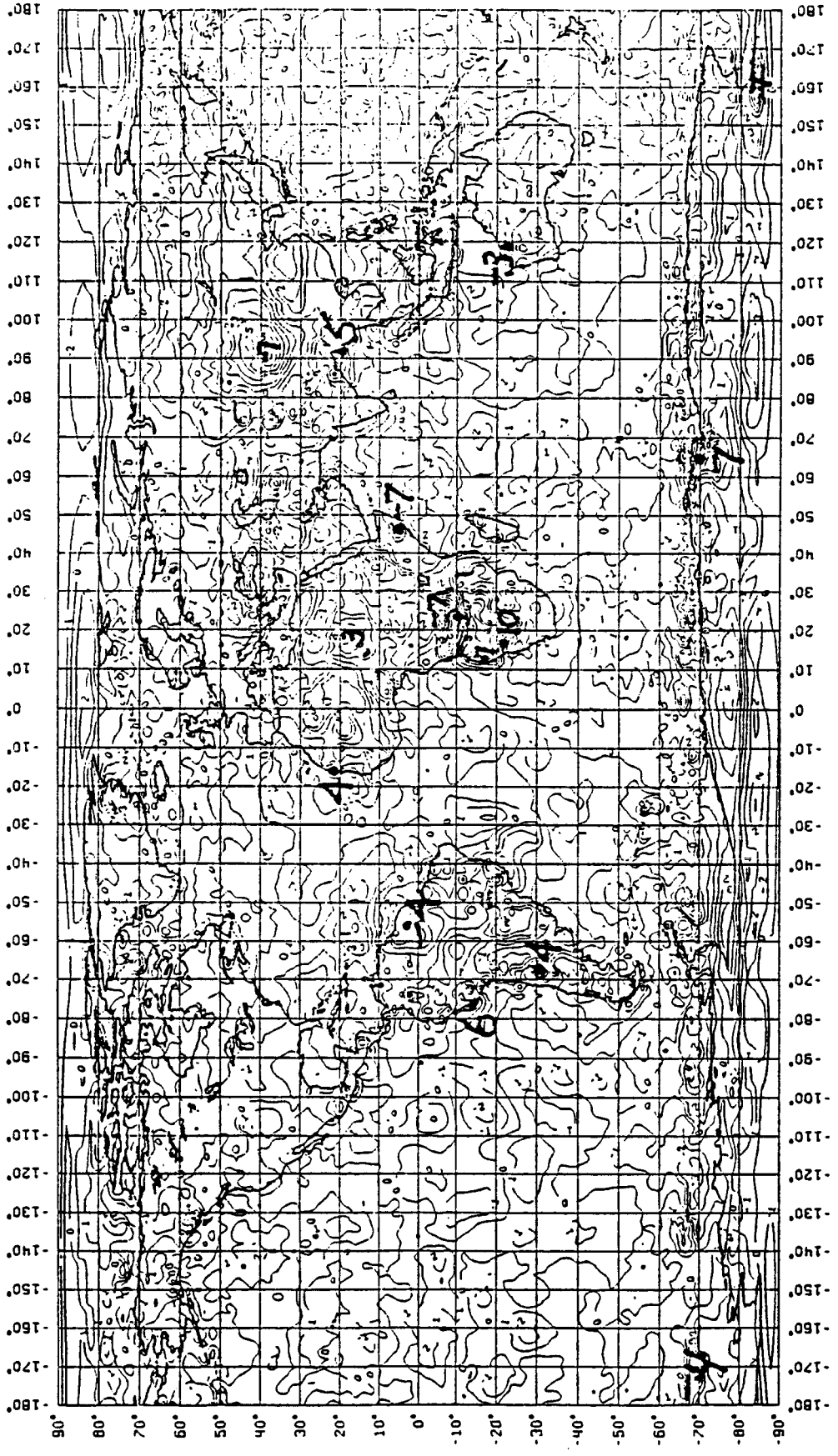

Figure 7. Geoid Undulation Differences (OSU86F - OSU81) Contour Interval = 1 m; 2°x2° Grid.

10. Conclusions

This report has described the estimation of an expansion of the earth's gravitational potential to degree 360. The method used, did not rigorously combine, satellite and terrestrial gravity data. Instead, we built on solutions that were formed using 1°x1° anomalies. We used a 30' data base formed from the merger of the anomalies derived from satellite altimetry in the oceans and terrestrial data for some land areas. Many land areas have no coverage or coverage only in terms of 1°x1° anomaly estimates. In such areas the field will not represent the high frequency variations that may actually exist in the area.

An important part of the anomaly reduction process is the downward continuation of the surface anomalies to the ellipsoid. In dealing with the 1° data we used a two term Taylor series involving a preliminary high degree field. We did not compute the downward continuation effects for the 30' cells. Instead we effectively used for each 30' cell the value used in the 1° reductions. Future solutions should examine improved techniques to carry out this downward continuation process.

We did not compute accuracy estimates for the coefficients. Such estimates would require a number of assumptions that would be unrealistic in practice. More work needs to be done in this area.

The next generation of the 360 field could involve the formal adjustment of the 30' mean anomalies and satellite data. More complete downward continuation procedures could be attempted. Accuracy evaluation should be of high importance.

Although there are a number of improvements that could be made for the next solution, the current solution appears to represent the given data and external data (e.g. Doppler undulations) quite well. We must remember, that just because we have a high degree field, it does not mean we have a highly accurate high degree field. The latter type of field will only be available when more precise data, such as would come from the Geopotential Research Mission of NASA (1986) would become available. Until then our solutions to 360 can be used for a number of purposes including realistic simulations for the GRM mission.

References

Colombo, O.L., Numerical Methods for Harmonic Analysis on the Sphere, Report No. 310, Dept. of Geodetic Science, The Ohio State University, Columbus, 1981.

Cruz, J.Y., Ellipsoidal Corrections to Potential Coefficients Obtained from Gravity Anomaly Data on the Ellipsoid, Report No. 371, Dept. of Geodetic Science and Surveying, The Ohio State University, Columbus, August 1986.

Despotakis, V., The Development of the June 1986 1°x1° and the August 1986 30'x30' Terrestrial Mean Free-Air Anomaly Data Bases, Internal Report, Dept. of Geodetic Science and Surveying, The Ohio State University, Columbus, OH, 1986.

Forsberg, R., Spectral Properties of the Gravity Field in the Nordic Countries, 1986.

Gleason, D., Partial sums of Legendre series via Clenshaw summation, manuscripta geodaetica, Vol. 10, No. 2, 115-130, 1985.

Hajela, D.P., Optimal Estimation of High Degree Gravity Field from a Global Set of 1°x1° Anomalies to Degree and Order 250, Report No. 358, Dept. of Geodetic Science and Surveying, The Ohio State University, Columbus, 1984.

Lerch, F.J., S. Klosko, and G. Patel, A Refined Gravity Model from Lageos (GEM-L2) Geophys. Res. Lett. 9, No. 11, 1263-1266, 1982.

NASA, Geopotential Research Mission, Science, Engineering, and Program Summary, NASA Technical Memorandum 86240, Goddard Space Flight Center, Greenbelt, MD 20771, May 1986.

Paul, M.K., Recurrence Relations for Integrals of the Associated Legendre Functions, Bulletin Geodesique, 52, 177-190, 1978.

Rapp, R.H., The Earth's Gravity Field to Degree and Order 180 Using SEASAT Altimeter Data, Terrestrial Gravity Data, and Other Data, Report No. 322, Dept. of Geodetic Science and Surveying, The Ohio State University, Columbus, Dec. 1981.

Rapp, R.H., Gravity Anomalies and Sea Surface Heights Derived from a Combined Geos 3/Seasat Altimeter Data Set, J. Geophys. Res., 91, 4867-4876, 1986.

Rapp, R., and J. Cruz, The Representation of the Earth's Gravitational Potential in a Spherical Harmonic Expansion to Degree 250, Report No. 372, Dept. of Geodetic Science and Surveying, The Ohio State University, Columbus, September 1986.